

# A New Type of Lightweight Low-Frequency Electromagnetic Hyperthermia Applicator

REG H. JOHNSON, ALAN W. PREECE, J. W. HAND, AND J. R. JAMES

**Abstract** — A new applicator is described which consists of a resonant circuit formed from a current-carrying sheet in the absence of a ground plane and which can be easily matched to a coaxial feeder. Designs for operation at frequencies in a range exceeding 10 to 1000 MHz are possible, and aperture dimensions can be chosen almost independently of frequency.

## I. INTRODUCTION

THE TREATMENT of tumors by hyperthermia depends on achieving effective penetration of electromagnetic energy into high-water-content tissue such as muscle. Such penetration ( $e^{-2}$  electric field) for a plane wave is approximately 3 cm at 900 MHz and 15 cm at 27 MHz. For deep-seated tumors it is desirable to employ frequencies of the order of 27 to 100 MHz and to make the aperture size of the radiator applicator sufficiently large to obtain the benefit of the increased penetration possible [1], [2]. Dielectric-loaded- and ridged-waveguide-type applicators are massive and relatively difficult to use at these frequencies. Simple capacitive methods employing two or more electrodes can operate at frequencies at or below 27 MHz [3] and can produce an electric field in intervening tissue. However, care is needed to prevent hot spots near the periphery of the small electrodes, and excessive heating of fat layers is likely because the electric field is normal to the fat layers.

Inductive applicators consisting of solenoids or pancake coils tuned by capacitors to operate at frequencies below or near 27 MHz produce nonuniform heating patterns and can produce hot spots due to the electric field between turns [3]. An alternative approach described by Andersen *et al.* [4] uses an inductive applicator consisting of current-carrying conductors above a ground plane, tuned by capacitors for resonance at 150 MHz. This has been shown to overcome the excessive surface heating associated with capacitor or coil systems. The idea has been extended to 27 MHz by Franconi *et al.* [5] in a linear induction applicator. The present paper describes a new type of radiator [6] which does not use a ground plane and which does not suffer from any of the above limitations.

Manuscript received April 3, 1987; revised August 9, 1987.

R. H. Johnson and J. R. James are with the Royal Military College of Science, Shrivenham, U.K.

A. W. Preece is with the Radio Therapy and Oncology Centre, Bristol Royal Infirmary, Bristol BS2 8ED, England.

J. W. Hand is with Hammersmith Hospital, London, England.

IEEE Log Number 8717107.

## II. DESIGN AND MODELING OF APPLICATOR PERFORMANCE

The energy absorbed from an electromagnetic wave by a lossy medium is  $E^2\sigma$ , where  $E$  is the electric field and  $\sigma$  is the conductivity. The electric field produces both ohmic current loss and dielectric loss. The electric field results from the magnetic field  $H$  and is given by

$$\nabla \times H = E(j\omega\epsilon + \sigma)$$

where  $\epsilon$  is the permittivity of the medium.

An antenna such as a current-carrying conductor produces a magnetic field and a corresponding electric field at any point depending on the geometry and the surrounding medium. The concept of the new applicator is a current sheet with the electromagnetic field mainly confined to one side by the circuit arrangement and screening. It consists of a flat high-conductivity plate folded back to form a U. Capacitor plates between the arms of the U form a resonant circuit, as shown diagrammatically in Fig. 1. This resonant circuit is enclosed in a screening box with an aperture covered by a suitable low-loss dielectric. Fig. 1(a) shows how the circuit can be excited by an inductive coupling loop, the rotation of which matches the coaxial input. Rotation of a high-conductivity plate adjacent to the coupling loop provides about 10 percent frequency adjustment. This arrangement is suitable for frequencies of about 100 MHz and below, whereas at higher frequencies the construction shown in Fig. 1(b) is suitable. Here, rotation of a split conducting disk connected to the coaxial input varies the input coupling to either side of the resonant circuit without appreciably affecting the resonant frequency. The latter is varied by moving the split disk either nearer to or further from the two half-plates which form part of the resonant circuit capacitance.

The resonant frequency is dependent on the value of the capacitance between the arms of the U and on the area of the loop formed by the U and that capacitance. For a given length of U-shaped radiating surface in the direction of current flow, the frequency can be changed either by altering the distance between the capacitance and the radiating plate or by altering the number of capacitor plates or the spacing between them. The resonant frequency is insensitive to the width of the radiating surface so long as this width and that of the capacitor plates remain in the same proportion.

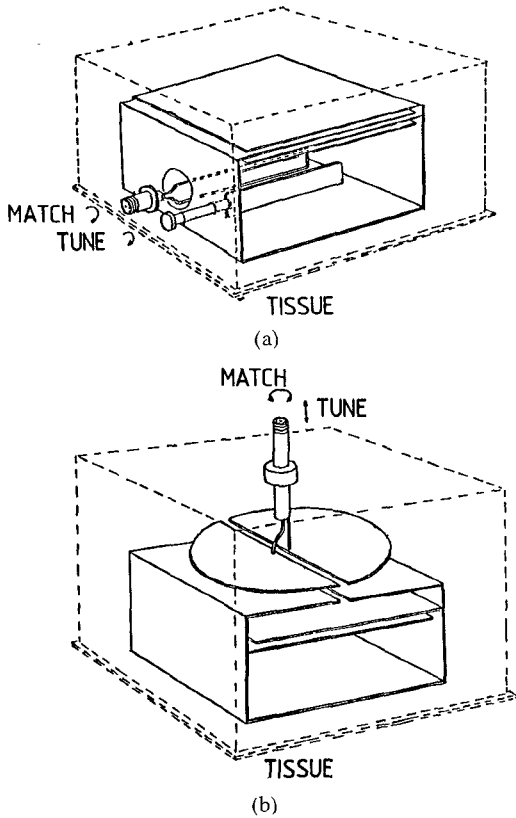


Fig. 1. Applicator construction. (a) Below about 100 MHz. (b) Above about 100 MHz.

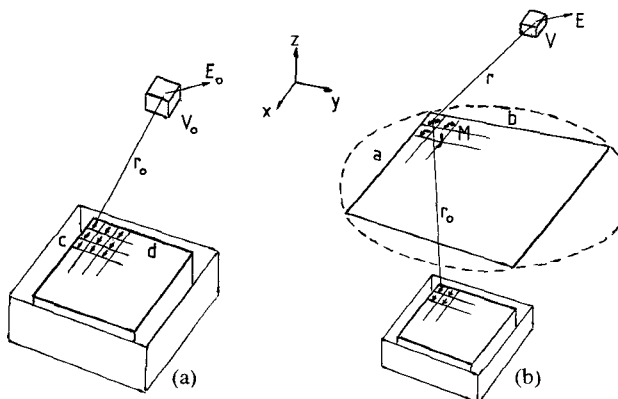


Fig. 2. Computation of applicator performance.

The high  $Q$ -factor resonant circuit is contained in a screening box and electromagnetic energy is radiated primarily from the current in the high-conductivity plate forming the base of the U. This current is assumed to be uniformly distributed normal to the current direction (across the width of the plate) and to have a sinusoidal component of amplitude in the current direction, as shown in Fig. 2.

The electric field  $E_0$  and hence the energy absorption in an elemental volume  $V_0$  of lossy medium distance  $r_0$  from a surface current element  $I dx dy$  in the radiating flat plate (Fig. 2(a)) are obtained from the vector potential  $A_0$  at  $V_0$ :

$$\vec{A}_0 = \frac{\mu}{4\pi} \int_{-c/2}^{c/2} \int_{-d/2}^{d/2} I \frac{e^{-jkr_0}}{r_0} dx dy \hat{x}$$

where  $\hat{x}$  is the unit vector in the current direction,  $k$  is the wavenumber in the medium, and  $\mu$  is the permeability of the medium. The planar current region is a rectangular surface of dimensions  $c \times d$ .

Hence the magnetic field  $H_0$  at  $V_0$  is given by

$$\vec{H}_0 = \frac{1}{\mu} \nabla \times \vec{A}_0$$

and the resulting electric field  $E_0$  is

$$\vec{E}_0 = \frac{1}{j\omega\epsilon} \nabla \times \vec{H}_0$$

where  $\epsilon$  is the permittivity of the medium and  $\omega$  is the angular frequency.

Energy loss in the elemental volume  $V_0$  is  $E_0^2\sigma$ , where  $\sigma$  is the conductivity of the medium. This value becomes more approximate at lower frequencies as the loss due to conduction current, which is affected by the geometry of the lossy medium, increases in comparison with the dielectric loss.

When the applicator is spaced from the lossy medium by air, dielectric, or bolus of significant thickness, it is first necessary to calculate the surface electric and magnetic fields ( $\vec{E}_s, \vec{H}_s$ ) in elemental areas of the interface plane between the media. These fields are then represented by fictitious magnetic and electric surface currents  $\vec{M}, \vec{J}$  according to the equivalence principle, giving

$$\vec{M} = -\hat{n} \times \vec{E}_s$$

$$\vec{J} = \hat{n} \times \vec{H}_s$$

where  $\hat{n}$  is the unit vector normal to the surface.

The magnetic and electric vector potentials  $\vec{A}, \vec{F}$  in an elemental volume  $V$  of the medium a distance  $r$  from a surface current element are given by

$$\vec{A} = \frac{\mu}{4\pi} \int_{-a/2}^{a/2} \int_{-b/2}^{b/2} (J_x \hat{x} + J_y \hat{y}) \frac{e^{-jkr}}{r} dx dy$$

$$\vec{F} = \frac{\epsilon}{4\pi} \int_{-a/2}^{a/2} \int_{-b/2}^{b/2} (M_x \hat{x} + M_y \hat{y}) \frac{e^{-jkr}}{r} dx dy$$

where  $a, b$  are the dimensions of the interface plane such as bolus/tissue, as indicated in Fig. 2(b).

The total electric field in  $V$ ,  $\vec{E}$ , is the sum of the electric fields  $\vec{E}_A$  and  $\vec{E}_F$  due to  $\vec{A}$  and  $\vec{F}$ , respectively, and since the magnetic field  $\vec{H}$  due to  $\vec{A}$  is  $-\frac{1}{\mu} \nabla \times \vec{A}$ ,

$$\vec{E}_0 = \vec{E}_A + \vec{E}_F = \frac{1}{j\omega\epsilon} \nabla \times \vec{H} - \frac{1}{\epsilon} \nabla \times \vec{F}.$$

Hence power absorption is  $E^2\sigma$ . Normally  $E_A \gg E_F$ .

### III. RESULTS

Table I lists examples of the new design and demonstrates that operating frequency and aperture dimensions can be chosen almost independently. This relationship is only constrained by the physical need to limit the length of the resonant plate to less than about one fifth of the free-space wavelength and by the practical difficulty of

TABLE I  
EXAMPLES OF THE NEW LIGHTWEIGHT APPLICATORS

Applicator	A**	B**	C*	D*	E*	F*	G*	H*
Frequency (MHz)	27	100	200	400	200/400/900			900
Radiator $L \times W$ (cm)	16 $\times$ 16	10 $\times$ 8.7	10 $\times$ 8.7	8 $\times$ 8		4 $\times$ 2.5		2.7 $\times$ 1.7
Aperture $L \times W$ (cm)	20 $\times$ 22	12.5 $\times$ 15.7	12.5 $\times$ 15.7	10 $\times$ 11.5		6.5 $\times$ 5		4 $\times$ 4
Height, net (cm)	10	9	10	5.5		4		4
Weight (kg)	4	0.7	0.9	0.4		0.2		0.1
Penetration ( $e^{-2}$ , cm)	6.7	4.1	3.5	2.9		1.6, 1.7, 1.7		1.6

\*Capacitive coupling.

\*\*Inductive coupling.

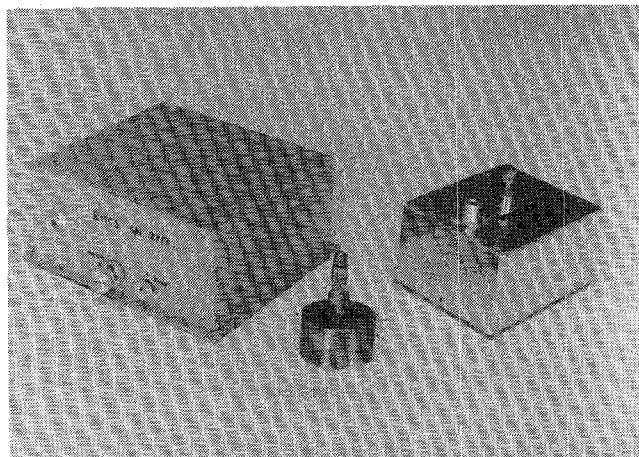


Fig. 3. Examples of the new applicators.

obtaining high values of capacitance without introducing unacceptable loss.

All the applicators listed in Table I use air as the dielectric, but solid (such as Teflon) or liquid (such as paraffin or carbon tetrachloride) dielectrics are possible. For continuous operation at the highest power levels, some cooling method may be necessary.

Fig. 3 illustrates examples of inductively and capacitively coupled applicators listed in Table I (applicators A and C), and also a compact version capable of operation over a wide range of frequencies (E, F, and G). This range is mainly achieved by using different values of capacitance in the tuned circuit—in this example a single size tunes 200–900 MHz with changed internal structure. All the applicators could be matched to 50- $\Omega$  coaxial input and tuned to the design frequency when applied to muscle phantom.

Fig. 4 shows the calculated heating patterns in muscle phantom for the 200 MHz (C) and 27 MHz (A) applicators. These are typical of all the applicators in Table I, which also lists the calculated penetration for muscle phantom ( $e^{-2}$  electric field).

Fig. 5 shows the impedance characteristics and return loss of the 200 MHz (C) and 27 MHz (A) applicators which are typical of this type of applicator. When unloaded, the applicator presents a high impedance and the

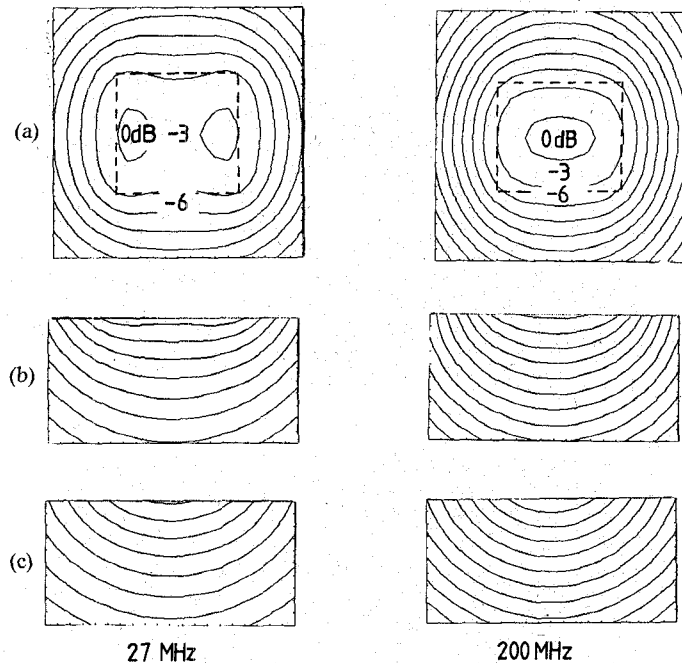


Fig. 4. Computed heating profiles of 200 MHz and 27 MHz applicators. (a) Central section parallel to current direction. (b) Central section normal to current direction. (c) Surface (parallel to applicator radiator, which is shown dotted).

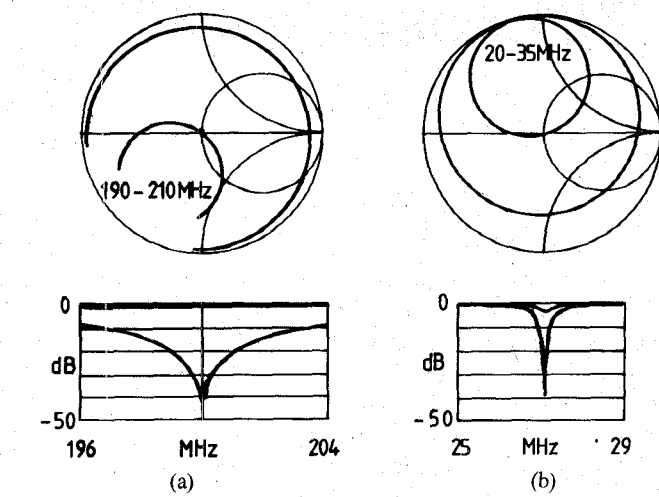


Fig. 5. Impedance and return loss of applicators. (a) 200 MHz. (b) 27 MHz.

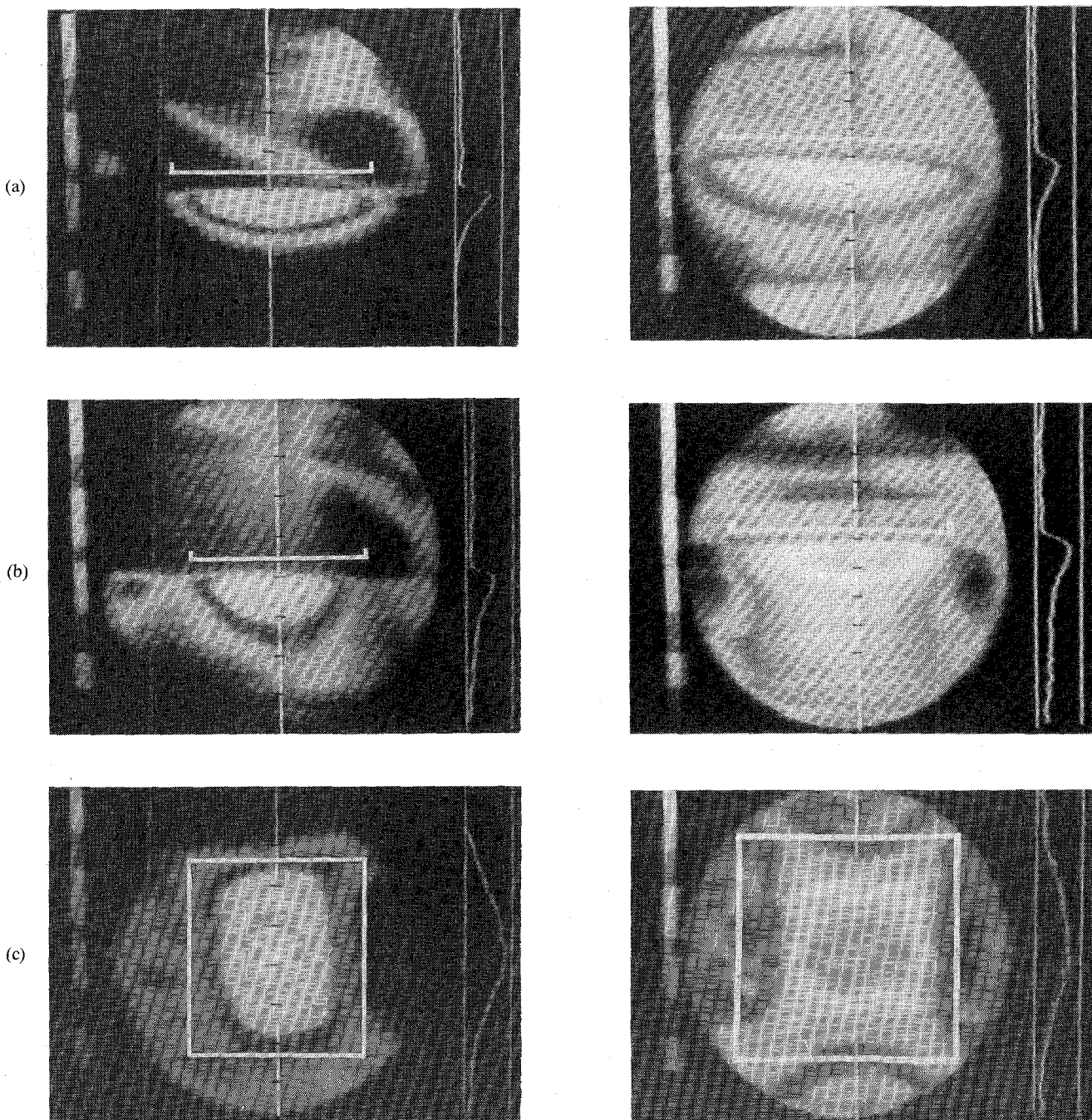


Fig. 6. Measured heating profiles of 200 MHz and 27 MHz applicators. False color scale—2°C per step. (a) Central section parallel to current direction. (b) Central section normal to current direction. (c) Surface (radiating area shown outlined).

power radiated is greatly reduced. Penetration depths have been measured by means of thermocouples or thermographic camera [7]. Results have been in good agreement with theory within the limits of measurement and phantom characteristics, but more especially the measured heating profiles follow closely the predicted patterns. This can be seen from Fig. 6(a) and (b), which shows the 200 MHz (C) and 27 MHz (A) applicator heating depth profiles parallel to and normal to the direction of current flow obtained by the split phantom technique. Fig. 6(c) shows the surface heating profile. These heating profiles were not signifi-

cantly affected by the applicator-phantom spacing or the presence of a water bolus. No hot spots have been observed.

At frequencies below about 200 MHz for muscle phantom, where energy absorption due to conduction currents would be expected to predominate, such currents would circulate and require a return path as described by Franconi *et al.* [5], thereby contributing to heating at some distance from the applicator with an intermediate null zone. With phantoms relatively large compared with the applicator aperture, these effects have not been observed but could be

present at low level. However this effect may be masking the extra heating calculated to occur but not observed near the ends of the current sheet at 27 MHz, as shown in Fig. 3. The induced conduction currents near the phantom surface are a function of the total induced electromotive force and the circuit impedance and will tend to be uniform near the applicator. Consequently, a more uniform surface heating profile will result, particularly at the lower frequencies, compared with that calculated ignoring this effect.

The measurements reported above refer to muscle phantom and show that the applicator produces heating profiles similar to those obtained with comparable conventional applicators. Power handling capabilities of all the applicators were compatible with the requirements of a clinical hyperthermia system. For example, the 27 MHz (A) and 200 MHz (C) applicators listed in Table I were tested up to input powers of 1 kW, which was the maximum available. According to Bassen and Coakley [8], an applicator should be capable of producing SAR values of 235 W/kg in the muscle region of a simulated muscle phantom. This value was obtained with input powers of 500 W and 155 W for applicators A and C, respectively. Kantor [9] reports a general loss of efficiency of applicators spaced from muscle tissue by air or increased fat layer thickness. The performance of the new applicators was found not to be significantly affected by reasonable thicknesses of the intervening material such as air, fat, or water bolus; this is due to the ease with which the applicators can be matched to the RF source and the inductive characteristics of the radiator.

An evaluation of the new applicator is being made on animals and patients, and it is well suited for multiple use in arrays, where its small size should make control of the heating profile relatively simple by adjustment of the amplitude/phase of the individual elements.

#### IV. CONCLUSIONS

The new lightweight applicator offers much greater frequency/size design flexibility than previously available for particular treatment sites.

It can be designed for a large range of sizes independently of frequency.

The applicator can be matched to tissue, irrespective of the permittivity, with reasonable thickness of the material between it and the muscle tissue to be heated, for example, fat or bolus.

Polarization is linear with electric field parallel to the aperture and consequently parallel to fat muscle interface.

It does not produce hot spots and can be operated at high power.

The applicator is inexpensive and can be used individually or in multiple arrays.

#### ACKNOWLEDGMENT

The authors would like to thank J. L. Murfin for her invaluable assistance in the preparation of this paper.

#### REFERENCES

- [1] P. F. Turner and L. Kumar, "Computer solution for applicator heating pattern," National Cancer Institute Monograph, 61, pp. 521-523, 1982.
- [2] R. H. Johnson, G. Andrasic, D. L. Smith, and J. R. James, "Field penetration of arrays of compact applicators in localised hyperthermia," *Int. J. Hyperthermia*, vol. 1, pp. 321-336, 1985.
- [3] J. W. Hand and R. H. Johnson, "Field penetration from electromagnetic applicators for localised hyperthermia," *Recent Results in Cancer Research*, vol. 101, pp. 7-17, 1986.
- [4] J. B. Andersen, A. Baun, K. Harkmark, P. Rashmark, and J. Overgaard, "A hyperthermia system using a new type of inductive applicator," *IEEE Trans. Biomed. Eng.*, vol. BME-31, pp. 21-27, 1984.
- [5] C. Franconi, C. Tiberio, L. Raganello, and L. Bernozzi, "Low frequency RF twin dipole applicator for intermediate depth hyperthermia," *IEEE Trans. Biomed. Eng.*, vol. BME-34, pp. 612-619, 1986.
- [6] R. H. Johnson, "New type of compact electromagnetic applicator for hyperthermia in the treatment of cancer," *Proc. Inst. Elec. Eng.*, vol. 22, pp. 591-593, 1986.
- [7] A. W. Preece and J. L. Murfin, "The use of an infrared camera for imaging the heating effect of RF applicators," *Int. J. Hyperthermia*, vol. 3, no. 2, pp. 119-122, 1987.
- [8] H. I. Bassen and R. F. Coakley, "United States radiation safety and regulatory considerations for radiofrequency hyperthermia systems," *J. Microwave Power*, vol. 16, pp. 215-226, 1981.
- [9] G. Kantor, "Evaluation and survey of microwave and radiofrequency applicators," *J. Microwave Power*, vol. 16, pp. 135-150, 1981.

✖

Reg H. Johnson was born in 1920 in England. He received the B.Sc. degree (first hons.) in electrical engineering and the M.Sc. degree from the University of Birmingham.

He retired from the Royal Radar Establishment, Malvern, in 1981 after research and development of various radar and guided weapon systems and related work. Following four years research on hyperthermia devices at the Royal Military College of Science, Shrivenham, he became a Consultant to the Wolfson RF Engineering Centre at RMCS, and is now a Consultant to the Radiotherapy Centre, Bristol.

✖

Alan W. Preece was born in 1940 in England, and obtained the B.Sc. degree in zoology in Bristol, and the Ph.D. degree on biological effects of radiation in 1966.

He has worked in cancer research for 21 years at the Radiotherapy Centre, Bristol, as a Principal Physicist, taking a particular research interest in nonionizing radiation. Now he is especially interested in tumor diagnosis and imaging using RF.

✖

J. W. Hand photograph and biography unavailable at the time of publication.

✖

J. R. James photograph and biography unavailable at the time of publication.